International Journal of Modern Physics C
Vol. 24, No. 4 (2013) 1350021 (19 pages)

DOI: 10.1142/S0129183113500216

ON SIMULATIONS OF HIGH-DENSITY RATIO FLOWS USING COLOR-GRADIENT MULTIPHASE LATTICE BOLTZMANN MODELS

HAIBO HUANG[*,§], JUN-JIE HUANG[†], XI-YUN LU[*]
and MICHAEL C. SUKOP[‡]

[*]*Department of Modern Mechanics*
University of Science and Technology of China
Hefei 230026, P. R. China

[†]*Department of Engineering Mechanics*
Chongqing University, Chongqing 400044, P. R. China

[‡]*Department of Earth and Environment*
Florida International University
Miami, Florida 33199, USA
[§]*huanghb@ustc.edu.cn*

Received 27 September 2012
Accepted 7 February 2013
Published 11 April 2013

Originally, the color-gradient model proposed by Rothman and Keller (R−K) was unable to simulate immiscible two-phase flows with different densities. Later, a revised version of the R−K model was proposed by Grunau *et al.* [D. Grunau, S. Chen and K. Eggert, Phys. Fluids A: Fluid Dyn. 5, 2557 (1993).] and claimed it was able to simulate two-phase flows with high-density contrast. Some studies investigate high-density contrast two-phase flows using this revised R−K model but they are mainly focused on the stationary spherical droplet and bubble cases. Through theoretical analysis of the model, we found that in the recovered Navier−Stokes (N−S) equations which are derived from the R−K model, there are unwanted extra terms. These terms disappear for simulations of two-phase flows with identical densities, so the correct N−S equations are fully recovered. Hence, the R−K model is able to give accurate results for flows with identical densities. However, the unwanted terms may affect the accuracy of simulations significantly when the densities of the two fluids are different. For the simulations of spherical bubbles and droplets immersed in another fluid (where the densities of the two fluids are different), the extra terms may not be important and hence, in terms of surface tension, accurate results can be obtained. However, generally speaking, the unwanted term may be significant in many flows and the R−K model is unable to obtain the correct results due to the effect of the extra terms. Through numerical simulations of parallel two-phase flows in a channel, we confirm that the R−K model is not appropriate for general two-phase flows with different densities. A scheme to eliminate the unwanted terms is also proposed and the scheme works well for cases of density ratios less than 10.

Keywords: Two-phase flows; two-component flows; lattice Boltzmann; R−K; density ratio.

1. Introduction

Numerous macroscopic numerical methods have been developed for solving the two-phase Navier−Stokes (N−S) equation,[1] such as the front-tracking method, the volume-of-fluid (VOF) method, the level set method, and so on. The former three methods are the most popular ones. However, the front-tracking method is usually not able to simulate interface coalescence or breakup.[1,2] In the VOF and level set methods, usually an interface reconstruction step or interface reinitialization is required, which may be nonphysical or complex to implement.[2] In addition, numerical instability may appear when the VOF and level set methods are applied to simulate surface-tension-dominated flows in complex geometries.[1]

In the last 20 years, the Lattice Boltzmann method (LBM) has been developed into a good tool to solve two-phase flows.[3−9] The LBM is a mesoscopic method and easily handles complex wall geometries. The LBM is an explicit method, which makes the code easy to parallelize. In the LBM, solving the Poisson equation is not required, hence it is more efficient than common macroscopic schemes.

There are many multiphase LBMs available in the literature, such as the Shan-Chen model,[10] free energy model,[11] Rothman−Keller model (R−K),[12] and so on.[9] The Shan-Chen multiphase model is the simplest one.[3] However, quantitative numerical study shows the model is not accurate[13] due to the inaccurate forcing term used in the model.[14] Using the correct forcing term in the Shan-Chen model, it is able to simulate two-phase flows with maximum density contrast of several hundred.[14]

The first multicomponent lattice gas model was proposed by Rothman and Keller.[12] The model was further developed by Gunstensen *et al.*[15] They introduced an extra binary fluid collision (perturbation operator) into the Lattice Boltzmann equation. Later, by introducing two free parameters in the rest equilibrium distribution function (DF), Grunau *et al.*[16] claimed the improved R−K model was able to simulate flows with different densities. Latva-Kokko and Rothman[17] improved the recoloring step in the R−K model, which is able to reduce the lattice pinning effect and decrease the spurious currents.[2,18] Now the recoloring step is widely used in applications of the R−K model.[2,13,19] Recently, Reis and Phillips developed a two-dimensional nine-velocity R−K model.[20] In the model, a revised binary fluid collision is proposed and is shown to be able to recover the term which accounts for surface tension in the N−S equations.[20] In some studies,[21,22] the forcing term strategy is used to introduce the surface tension instead of the perturbation operator. Here we still adopt the perturbation operator because it is regarded as one of main characteristics of the R−K model.

First we review the evidence in the literature that the R−K model is able to handle high-density ratio two-phase flows. In almost all validations,[16,23,24] only cases of stationary bubbles or droplets[16,23,24] are simulated. Usually, the studies[16,23,24] used the Laplace law to calculate the surface tension and compared with the analytical value. In Ref. 24, a density ratio between the fluids as high as 10 000 is simulated. In addition to the cases of stationary droplet and bubble simulations, rising bubble

cases[2,23,25] are also used to perform validation of the R−K method to some extent. However, usually only density ratios less than 4 are simulated.[2,20,23,25]

In the literature, it is more often that cases with identical densities were simulated using the R−K model, such as droplet deformation and breakup in simple shear flow,[2] two-phase flow in porous media,[4] high-viscosity ratio two-phase parallel flow in a channel.[18,25] Note in the latter two flows, only two fluids with identical densities but different kinematic viscosities are simulated.

Hence, it is uncertain that whether the R−K model is able to simulate two-phase flows with high-density ratios beyond the stationary droplet and bubble cases. Rothman [personal communication], who invented the R−K model indicated that "As for the case of different densities, these models[17,19] do not perform so well. You may find some useful alternative algorithms (e.g. Shan and Chen)." Hence, according to Rothman's opinion, for flows with different densities, usually the R−K model does not perform as well as other multiphase LBMs.

Recently, some numerical studies also reported that the R−K model gave poor results for two-phase parallel flows with different densities in a channel.[26] Although the thesis[26] demonstrated the incorrect results, it is still unknown why the model is unable to give correct results. In this paper, through analysis of the recovered macroscopic equations, some extra terms are found in the recovered momentum equation. These extra terms may affect the numerical results significantly. For example, due to these terms, the tangential shear stress condition in the interface vicinity is not satisfied properly. For the cases of stationary bubble or droplet, the extra terms may be negligible and it does not affect the result much in terms of surface tension.

The paper is arranged in the following way. The R−K model is introduced briefly. Through theoretical analysis, we show that usually the R−K model introduces some extra unwanted terms in the recovered macroscopic momentum equation. For two-phase flows with different densities, the terms are usually unable to be eliminated. Through numerical study of two-phase parallel flows in a channel, we confirm that the R−K model for different density ratios is usually incorrect except for the stationary droplet and bubble cases. A scheme to eliminate the unwanted terms is proposed and evaluated.

2. Method

2.1. *R−K model*

In the R−K model, the particle distribution function (PDF) for fluid k is defined to be f_i^k. For two-phase flows, two DFs are defined, i.e. f_i^b, and f_i^r, where b and r denote "blue" or "red" component. The total PDF at $(\mathbf{x}, \mathbf{t})$ is $f_i(\mathbf{x}, \mathbf{t}) = \sum_k f_i^k(\mathbf{x}, \mathbf{t})$.

Usually there are two steps implemented in the LBM, collision and streaming. In the R−K model, there are three steps for each component: streaming, collision and recoloring. Suppose an iteration begins from the streaming step. We illustrate

how the three steps construct a loop. The streaming step is[20]

$$f_i^k(\mathbf{x}+\mathbf{e}_i\delta t, t+\delta t) = f_i^{k+}(\mathbf{x}, t), \tag{1}$$

where f_i^{k+} is the PDF after the recoloring step. In the above equation, $\mathbf{e}_i, i = 0, 1, \ldots, b$ are the discrete velocities of the velocity models. For the D2Q9 velocity model ($b = 8$), they are

$$[\mathbf{e}_0, \mathbf{e}_1, \mathbf{e}_2, \mathbf{e}_3, \mathbf{e}_4, \mathbf{e}_5, \mathbf{e}_6, \mathbf{e}_7, \mathbf{e}_8] = c\begin{bmatrix} 0 & 1 & 0 & -1 & 0 & 1 & -1 & -1 & 1 \\ 0 & 0 & 1 & 0 & -1 & 1 & 1 & -1 & -1 \end{bmatrix}.$$

Here c is the lattice speed defined to be $c = \frac{\delta x}{\delta t}$. We use the lattice units of $\delta x = 1l.u.$ and $\delta t = 1t.s.$ in our study. Mass unit is denoted with $m.u.$

The collision step can be written as[17]

$$f_i^{k*}(\mathbf{x}, t) = f_i^k(\mathbf{x}, t) + (\Omega_i^k)^1 + (\Omega_i^k)^2, \tag{2}$$

where $f_i^{k*}(\mathbf{x}, t)$ is the post-collision state. There are two collision terms in the equation, i.e. $(\Omega_i^k)^1$ and $(\Omega_i^k)^2$. Here, the lattice BGK scheme is adopted, the first collision term is

$$(\Omega_i^k)^1 = -\frac{\delta t}{\tau}(f_i^k(\mathbf{x}, t) - f_i^{k,\mathrm{eq}}(\mathbf{x}, t)). \tag{3}$$

τ is the relaxation time.

The equilibrium DF $f_i^{k,\mathrm{eq}}(\mathbf{x}, t)$ can be calculated using[20]

$$f_i^{k,\mathrm{eq}}(\mathbf{x}, t) = \rho_k\left(C_i + w_i\left[\frac{\mathbf{e}_i \cdot \mathbf{u}}{c_s^2} + \frac{(\mathbf{e}_i \cdot \mathbf{u})^2}{2c_s^4} - \frac{(\mathbf{u})^2}{2c_s^2}\right]\right), \tag{4}$$

where the density of the kth component is $\rho_k = \sum_i f_i^k$, and the total density is $\rho = \sum_k \rho_k$. The momentum is $\rho\mathbf{u} = \sum_k \sum_i f_i^k \mathbf{e}_i$. In the above formula, the coefficients are[20] $C_0 = \alpha_k$, $C_i = \frac{1-\alpha_k}{5}, i = 1, 2, 3, 4$ and $C_i = \frac{1-\alpha_k}{20}, i = 5, 6, 7, 8$, where α_k is a parameter that is assumed able to adjust the density of fluids.[16,20] The density ratio is[16,20] $\kappa = \frac{\rho_r}{\rho_b} = \frac{1-\alpha_b}{1-\alpha_r}$. The other parameters are $w_0 = \frac{4}{9}$, $w_i = \frac{1}{9}, i = 1, 2, 3, 4$ and $w_i = \frac{1}{36}, i = 5, 6, 7, 8$.

When the relaxation time parameters for the two fluids are very different, for example, $\tau_r = 0.501$ and $\tau_b = 1.0$, $\tau(\mathbf{x})$ at the interface can be determined by a simple way: $\psi(\mathbf{x}) = \frac{\rho_r(\mathbf{x})-\rho_b(\mathbf{x})}{\rho_r(\mathbf{x})+\rho_b(\mathbf{x})} > 0$, $\tau(\mathbf{x}) = \tau_r$ and otherwise $\tau(\mathbf{x}) = \tau_b$. To make the relaxation parameter $(\tau(\mathbf{x}))$ change smoothly at the interfaces between two fluids, here we adopt the interpolation scheme constructed by Grunau *et al.*[16,20]

$$\tau = \begin{cases} \tau_r & \psi > \delta, \\ g_r(\psi) & \delta \geq \psi > 0, \\ g_r(\psi) & 0 \geq \psi \geq -\delta, \\ \tau_b & \psi < -\delta, \end{cases}$$

where $g_r(\psi) = s_1 + s_2\psi + s_3\psi^2$, $g_b(\psi) = t_1 + t_2\psi + t_3\psi^2$, and $s_1 = t_1 = 2\frac{\tau_r\tau_b}{\tau_r+\tau_b}$, $s_2 = 2\frac{\tau_r-\alpha}{\delta}$, $s_3 = -\frac{\beta}{2\delta}$, $t_2 = 2\frac{\alpha-\tau_b}{\delta}$ and $t_3 = \frac{\eta}{2\delta}$. Here $\delta \leq 1$ is a free positive parameter. The viscosity of each component is $\nu_k = c_s^2(\tau_k - 0.5)$, where $c_s^2 = \frac{1}{3}c^2$.

The second collision term is more complex and there are some different forms found in the literature.[13,20] An example is[13]:

$$(\Omega_i^k)^2 = \frac{A_k}{2}|\mathbf{f}|(2\cdot\cos^2(\lambda_i) - 1), \tag{5}$$

where λ_i is the angle between the color gradient $\mathbf{f}$ and the direction $\mathbf{e}_i$, and we have $\cos(\lambda_i) = \frac{\mathbf{e}_i\cdot\mathbf{f}}{|\mathbf{e}_i|\cdot|\mathbf{f}|}$.[17]

The color gradient $\mathbf{f}(\mathbf{x}, t)$ is calculated as[17]:

$$\mathbf{f}(\mathbf{x}, t) = \sum_i \mathbf{e}_i \sum_j [f_j^r(\mathbf{x} + \mathbf{e}_i\delta t, t) - f_j^b(\mathbf{x} + \mathbf{e}_i\delta t, t)]. \tag{6}$$

However, according to the study of Reis and Phillips,[20] the correct collision operator should be

$$(\Omega_i^k)^2 = \frac{A_k}{2}|\mathbf{f}|\left[w_i\frac{(\mathbf{e}_i\cdot\mathbf{f})^2}{|\mathbf{f}|^2} - B_i\right], \tag{7}$$

where $B_0 = -\frac{4}{27}$, $B_i = \frac{2}{27}, i = 1, 2, 3, 4$, $B_i = \frac{5}{108}, i = 5, 6, 7, 8$. Using these parameters, the correct term due to surface tension in the N−S equations can be recovered.[20]

Then the recoloring step is implemented to achieve separation of the two fluids,[17]

$$f_i^{r,+} = \frac{\rho_r}{\rho}f_i^* + \beta\frac{\rho_r\rho_b}{\rho^2}f_i^{(\mathrm{eq})}(\rho, 0)\cos(\lambda_i), \tag{8}$$

$$f_i^{b,+} = \frac{\rho_b}{\rho}f_i^* - \beta\frac{\rho_r\rho_b}{\rho^2}f_i^{(\mathrm{eq})}(\rho, 0)\cos(\lambda_i), \tag{9}$$

where $f_i^* = \sum_k f_i^{k*}$ and β usually takes any value between 0 and 1.[17]

After $f_i^r(\mathbf{x}, t)$, and $f_i^b(\mathbf{x}, t)$ are updated, the streaming steps [i.e. Eq. (1)] should be implemented for each component. Through iteration of the procedure illustrated above, two-phase flows can be simulated.

In the model, A_k, and β are the most important parameters that adjust interfacial properties. The interfacial thickness can be adjusted by β but the surface tension is independent of β and only determined by A_k and τ_r, τ_b.[17] The pressure in the flow field can be obtained from the density via the equation of state $p = c_s^2\rho$.

Note that when components with identical densities are considered, the corresponding equilibrium DF is Eq. (4) with $C_i = w_i$. That is the common equilibrium DF usually used in the LBM. Hence, when two components have identical densities, the equilibrium DF has the same formula. It is not necessary to calculate both collision steps Eqs. (3) and (7) separately for each component. The two collision steps become,

$$(\Omega_i)^1 = -\frac{\delta t}{\tau}(f_i(\mathbf{x}, t) - f_i^{\mathrm{eq}}(\mathbf{x}, t)), \tag{10}$$

and

$$(\Omega_i)^2 = A|\mathbf{f}|\left[w_i\frac{(\mathbf{e}_i\cdot\mathbf{f})^2}{|\mathbf{f}|^2} - B_i\right], \tag{11}$$

where $A = \sum_k A_k/2$ and $f_i = \sum_k f_i^k$.

3. Results and Discussion

3.1. *Theoretical analysis*

Here, we show that incorporation of the freedom of the rest particle equilibrium distribution in a revised R−K model[16] generally fails to recover the correct N−S equations.

In the following derivatives, because the collision step $(\Omega_i^k)^2$ is not considered, the surface tension does not appear. The derivation in the Ref. 20 demonstrates that the term incorporating the surface tension in the recovered macroscopic momentum equation is only introduced by $(\Omega_i^k)^2$. The collision step $(\Omega_i^k)^2$ does not affect the other terms in the derived momentum equation [see Eq. (17)].[20]

The study of Liu *et al.*,[2] included the derivation of the N−S equations in the single-phase region. Now we focus on Eq. (A14) in Ref. 2, i.e. the first-order momentum flux tensor

$$\begin{aligned}\Pi_{\alpha\beta}^{k,(1)} &= \sum_i f_i^{k,(1)} e_{i\alpha} e_{i\beta} = -\tau_k \sum_i e_{i\alpha} e_{i\beta} D_{t0} f_i^{k,eq} \\ &= -\tau_k \left\{ \partial_{t0}(\rho_k u_\alpha u_\beta + p_k \delta_{\alpha\beta}) + \partial_\gamma \left[\frac{1}{3} \rho_k c^2 (u_\alpha \delta_{\beta\gamma} + u_\beta \delta_{\gamma\alpha} + u_\gamma \delta_{\alpha\beta}) \right] \right\}, \quad (12)\end{aligned}$$

where $D_{t0} \equiv (\partial_{t0}) + e_{i\gamma}\partial_\gamma$.

Then we substitute the following continuity equation [see Eq. (13)] and Euler equation [see Eq. (14)], which was obtained from the Chapman−Enskog expansion,[2] into the above equation [see Eq. (12)].

$$\partial_{t0}\rho_k = -\partial_\gamma(\rho_k u_\gamma), \quad (13)$$

$$\partial_{t0}(\rho_k u_\alpha) = -\partial_\beta(\rho_k u_\alpha u_\beta + p_k \delta_{\alpha\beta}), \quad (14)$$

where $p_k = (c_s^k)^2 \rho_k$ and $(c_s^k)^2 = \frac{3}{5}(1 - \alpha_k)$.

If omitting the terms of $O(u^3)$, such as $u_\beta \partial_\gamma(\rho_k u_\alpha u_\gamma)$ and so on, we have,

$$\begin{aligned}\Pi_{\alpha\beta}^{k,(1)} &= -\tau_k \left\{ u_\beta \partial_{t0}(\rho_k u_\alpha) + u_\alpha \partial_{t0}(\rho_k u_\beta) - u_\alpha u_\beta \partial_{t0}\rho_k + (c_s^k)^2 (\partial_{t0}\rho_k \delta_{\alpha\beta}) \right. \\ &\quad \left. + \partial_\gamma \left[\frac{1}{3} \rho_k c^2 (u_\alpha \delta_{\beta\gamma} + u_\beta \delta_{\gamma\alpha} + u_\gamma \delta_{\alpha\beta}) \right] \right\} \\ &= -\tau_k \left\{ -(c_s^k)^2 \left[u_\beta \partial_\alpha(\rho_k) + u_\alpha \partial_\beta(\rho_k) + \partial_\gamma(\rho_k u_\gamma)\delta_{\alpha\beta} \right] \right. \\ &\quad \left. + \frac{1}{3} c^2 \left[\partial_\beta(\rho_k u_\alpha) + \partial_\alpha(\rho_k u_\beta) + \partial_\gamma(\rho_k u_\gamma)\delta_{\alpha\beta} \right] \right\}. \quad (15)\end{aligned}$$

At this step, Ref. 2 obtained,

$$\begin{aligned}\Pi_{\alpha\beta}^{k,(1)} &= -\tau_k \left\{ \left[\frac{1}{3} c^2 - (c_s^k)^2 \right] \left[u_\beta \partial_\alpha(\rho_k) + u_\alpha \partial_\beta(\rho_k) + \partial_\gamma(\rho_k u_\gamma)\delta_{\alpha\beta} \right] \right\} \\ &\quad - \frac{1}{3} c^2 \tau_k \rho_k \left[\partial_\beta u_\alpha + \partial_\alpha u_\beta \right]. \quad (16)\end{aligned}$$

Finally, the macroscopic momentum equation recovered from the R−K model is,

$$\begin{aligned}&\partial_t(\rho_k u_\alpha) + \partial_\beta(\rho_k u_\alpha u_\beta)\\ &\quad = -\partial_\alpha p + \rho_k \nu_k \partial_\beta(\partial_\alpha u_\beta + \partial_\beta u_\alpha) + \left(\tau_k - \frac{1}{2}\right)\partial_\beta\\ &\qquad \times \left\{\left[\frac{1}{3}c^2 - (c_s^k)^2\right]\left[u_\beta \partial_\alpha(\rho_k) + u_\alpha \partial_\beta(\rho_k) + \partial_\gamma(\rho_k u_\gamma)\delta_{\alpha\beta}\right]\right\}. \end{aligned} \tag{17}$$

The term $\nu_k \partial_\beta(\partial_\alpha u_\beta + \partial_\beta u_\alpha)$ is the viscosity term that appears in the N−S equations and the recovered kinematic viscosity is $\nu_k = c_s^2(\tau_k - 0.5)$. Compared to the N−S equations, the last term in Eq. (17), i.e.

$$U_\alpha^k = \left(\tau_k - \frac{1}{2}\right)\left[\frac{1}{3}c^2 - (c_s^k)^2\right]\partial_\beta\{[u_\beta \partial_\alpha(\rho_k) + u_\alpha \partial_\beta(\rho_k) + \partial_\gamma(\rho_k u_\gamma)\delta_{\alpha\beta}], \tag{18}$$

is an unwanted extra term that appears in the momentum equations. In Ref. 2, it was assumed that the term is of $O(u^3)$. In single-phase flows, the density gradient is small and the assumption may be true. However, for the two-phase flows with different densities, $\frac{1}{3}c^2 \neq (c_s^k)^2$, and near the interface the density gradient $u_\beta \partial_\alpha(\rho_k)$ or $u_\alpha \partial_\beta(\rho_k)$ may be significant. Hence, the last term in Eq. (17) may be important and should not be neglected.

On the other hand, for the two-phase flows with identical densities, usually $C_i = w_i$ ($\alpha_k = \frac{4}{9}, k = 1, 2$) is adopted and $\frac{1}{3}c^2 = (c_s^k)^2$ is always valid. In this way, the undesired term would disappear automatically. Hence, the N−S equation is correctly recovered and the R−K model is always correct for two-phase flows with identical densities.

Here we propose a scheme to eliminate the unwanted extra terms. The terms can be regarded as forcing terms in the N−S equations. To eliminate the forcing terms in recovered macroscopic equation, we can introduce a source term into the lattice Boltzmann equation (LBE), i.e. S_i^k into Eq. (2).

$$S_i^k = -w_i U_\alpha^k e_{i\alpha} \frac{1}{c_s^2}. \tag{19}$$

With $\sum_i S_i^k = 0$, and $\sum_i e_{i\beta} S_i^k = -U_\beta^k$, we know that when this source term is added into LBE, the correct N−S equation for kth component is recovered. We also note that the forcing term in Eq. (19) is calculated explicitly through the density and velocity at last time step. Such a treatment cannot eliminate completely the error term in Eq. (17) for an unsteady flow problem.

To add the source term into LBE, one has to evaluate the density gradient and relevant derivatives in the above Eq. (18). For example, to evaluate $\partial_y \rho_r$ and $\partial_y(u_x \partial_y \rho_r)$ at a lattice node, we adopt the central finite difference method.

$$\begin{aligned}(\partial_y \rho_r)_{(i,j)} &= \frac{1}{2\delta_y}[(\rho_r)_{(i,j+1)} - (\rho_r)_{(i,j-1)}],\\ [\partial_y(u_x \partial_y \rho_r)]_{(i,j)} &= \frac{1}{2\delta_y}\left[(u_x)_{(i,j+1)}(\partial_y \rho_r)_{(i,j+1)} - (u_x)_{(i,j-1)}(\partial_y \rho_r)_{(i,j-1)}\right],\end{aligned} \tag{20}$$

where $\delta_y = 1l.u.$ and the subscript (i, j) denotes the column and row indices of a lattice node in the computational domain.

In the following, the cases of a droplet inside another fluid and parallel two-phase flows in a channel are simulated. We can see the extra terms is important; neglecting it may lead to incorrect results.

3.2. *Cases of a stationary droplet immersed in another fluid*

In the following study, the lattice units are used. The units of some parameters are listed in Table 1. Some other parameters, such as C_i, ω_i, α, β and A, are non-dimensional parameters.

In this section, cases of a droplet immersed in another fluid are simulated. In the simulations, we adopt $\beta = 0.99$ and $\tau_r = \tau_b = 1$, which is identical as that in the study of Leclaire[24] and $A_r = A_b = A = 10^{-4}$. In cases of density ratio $\kappa = \frac{\rho_r}{\rho_b} = \frac{1-\alpha_b}{1-\alpha_r} = \frac{0.8}{0.008} = 100$, $\alpha_b = 0.2$ and $\alpha_r = 0.992$. In cases of density ratio $\kappa = 1000$, $\alpha_b = 0.2$ and $\alpha_r = 0.9992$. For $\kappa = 1000$, three cases with different initial radii of the droplet are simulated and the results is shown in Table 2. In the table, the surface tension is calculated through the Laplace law: $\sigma = (p_{\text{in}} - p_{\text{out}})R$, where R is the final equilibrium radius of the droplet. The radius is measured from the center of the droplet to the contour of $\rho_r = 0.4 = \frac{0.8}{2}$. Here, we can see that the calculated surface tensions are all consistent with the analytical ones, i.e. $\sigma = \frac{4}{3}(1 + \frac{1}{\kappa}) \times \frac{\rho_r}{2}\tau = 1.07 \times 10^{-4}$ in Ref. 24.

The spurious currents near the interface for the case of $\kappa = 100$ are shown in Fig. 1. The right lower quarter of the droplets are shown. The density contours of $\rho_r = 0.7, \rho_r = 0.4$ and $\rho_r = 0.1$ are also shown in the figure with thick black lines. The result shows that the magnitude of the spurious velocity inside the density contours is about $10^{-5}\, l.u./t.s.$ Figure 1(b) shows that in the interface the spurious velocity forms some small vorticities. It is difficult to analyze why the R−K model works well for the stationary droplet in terms of surface tension value. It may be

Table 1. Units of parameters.

Variables	Unit	Variables	Unit
f_i, ρ	$m.u./(l.u.)^3$	p	$(m.u./l.u./(t.s.)^2)$
$\mathbf{u}, c_s$	$l.u./t.s.$	G, θ	$m.u./(l.u.)^2/(t.s.)^2$
τ	$t.s.$	σ	$(m.u./(t.s.)^2)$

Table 2. Simulations of stationary droplets with density ratio 1000 ($A = 10^{-4}, \beta = 0.99, \tau_r = \tau_b = 1$, $\alpha_b = 0.2$ and $\alpha_r = 0.9992$).

Case	Initial R	Equilibrium R	p_{in}	p_{out}	σ
(a)	15	14.97	3.9089e-4	3.8350e-4	1.108e-4
(b)	20	19.92	3.888e-4	3.8334e-4	1.093e-4
(c)	25	24.95	3.8752e-4	3.8317e-4	1.085e-4

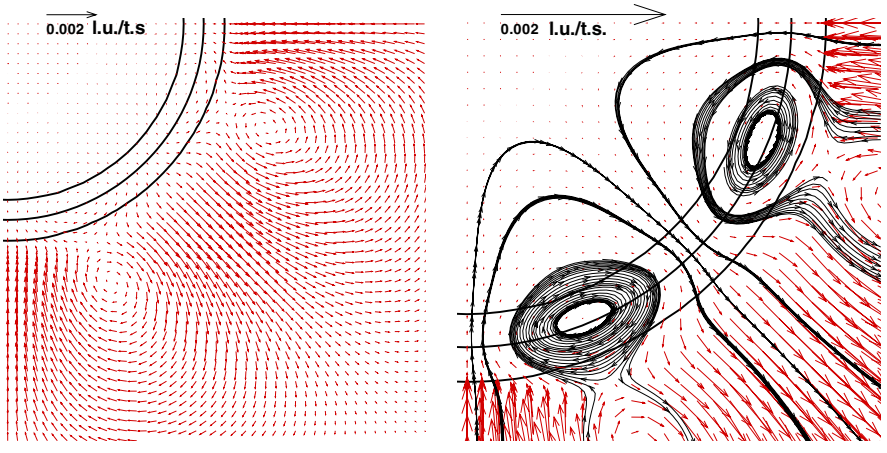

(a) (b)

Fig. 1. (Color online) Spurious velocity filed in the vicinity of the interface (a quarter of the circular droplet is shown), (a) density ratio $\kappa = 100$ ($\rho_r = 1 - \alpha_b = 0.8$ and $\rho_b = 1 - \alpha_r = 0.008$), (b) A zoom-in view of subfigure (a), streamlines in the interface vicinity are shown. The reference vector and density contours of $\rho_r = 0.7, \rho_r = 0.4$ and $\rho_r = 0.1$ (from the inside of the droplet to the outside) are also shown.

related to these vorticities in the interface. Due to these vorticities, the integral effect of the unwanted term may be canceled in some extent. Then the recovered momentum equation [see Eq. (17)] would be close to the N−S equations. We also tried the case with density ratio $\kappa = 10\,000$, the R−K model works well as mentioned in the Ref. 24.

Hence, our numerical results also demonstrate that the R−K model is able to simulate the cases of stationary droplets with high-density ratios correctly in terms of surface tension. This observation is highly consistent with the results in the literature.[16,20,23–25] However, it does not necessary mean the R−K is able to handle general high-density contrast two-phase flows correctly. In the following section, we investigate the performance of the R−K model for parallel two-phase flows in a channel.

3.3. *Layered two-phase flow in a 2D channel*

Here two-phase immiscible layered flows between two parallel plates are simulated. In the simulation, as illustrated in Fig. 2, periodic boundary conditions are applied on the left and right boundaries. For the lattice nodes in upper and lower plates, only simple bounce back is implemented and the collision steps are not implemented. It is noted that when simple bounce back is used to mimic the nonslip boundary condition, the wall is actually located halfway between a flow node and a bounce-back node.[27]

In this flow, the vertical velocity u_y is assumed to be zero everywhere inside the computational domain. Due to periodic boundary condition in x-direction, the

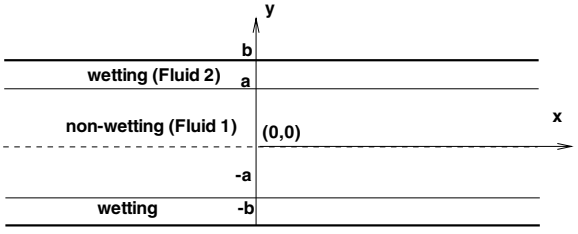

Fig. 2. Layered immiscible two-phase flow in a 2D channel. The wetting (fluid 2) phase flows along upper and lower plates while the nonwetting phase (fluid 1) flows in the center region.

derivatives in x-direction is zero, i.e. $\partial_x(\phi) = 0$, where ϕ denote density, velocity and pressure. Hence, in the steady flow, for k-component, the N−S equations [i.e. Eq. (17)] can be simplified as

$$\rho_k \nu_k \partial_y^2 u_x + G + (\tau_k - 0.5)\left[\frac{c^2}{3} - (c_s^k)^2\right]\partial_y(u_x \partial_y \rho_k) = 0, \tag{21}$$

where G denote the body force, which has identical unit as $\rho\partial_t u_x$ (refer to Table 1).

In our simulations, the nonwetting phase flows in the central region $0 < |y| < a$, while the wetting phase flows in the region $a < |y| < b$. Assuming the flow in the channel is Poiseuille-type, the analytical solution for the velocity profile between the parallel plates can be obtained.[6,26]

The computational domain is 10×100. Because the periodic boundary condition is used on the left and right boundaries, the number of mesh nodes used in x-direction can be much smaller. The error between numerical and analytical solutions is defined as

$$E(t) = \frac{\sum_j |u(j,t) - u_0(j)|}{\sum_j |u_0(j)|}, \tag{22}$$

where the summation is over the lattice nodes j in the slice $x = 5$, and u_0 is the analytical solution. The convergence criterion is $|\frac{E(t)-E(t-10^4\delta t)}{E(t-10^4\delta t)}| < 10^{-4}$.

Figure 3 shows the velocity profile across the middle vertical section of the channel for different kinematic viscosity ratios $M = \frac{\nu_{\rm nw}}{\nu_w} = \frac{\nu_1}{\nu_2}$, where $\nu_{\rm nw}$ and ν_w are the kinematic viscosities of nonwetting and wetting fluids, respectively. In the figure, velocity profiles in (a) and (b) are obtained through applying a body force $G = 1.5 \times 10^{-8}$ to both fluids. From Fig. 3, we can see that the numerical solutions agree well with the analytical ones. Here, the kinematic viscosity of component "k" is calculated with $\nu_k = c_s^2(\tau_k - 0.5)$. Applying the R−K model,[16,17] some studies of this flow[18,26] have shown that the numerical error would increase with viscosity ratio contrast but still agree well with the analytical solution. Here, we also observed this trend (not shown).

In Ref. 26, is was reported that, when the densities of the two fluids are different, the numerical results obtained through the R−K model for this flow do not agree with the analytical solution. Here we further confirmed this conclusion. Eight simulations (a1) to (d2) that are listed in Table 3 were performed. In the cases (a1),

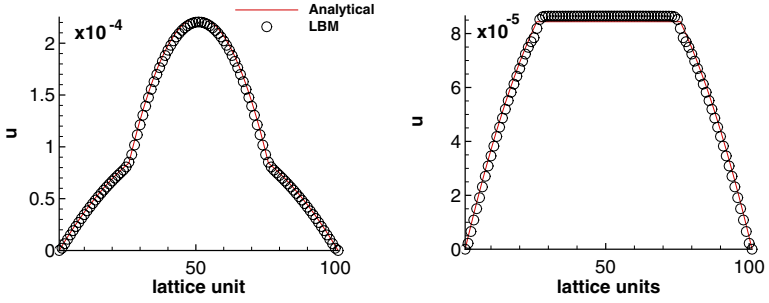

(a) (b)

Fig. 3. (Color online) Velocity profiles for cases with identical densities and $G = 1.5 \times 10^{-8}$, (a) $M = \frac{1}{5}$ and (b) $M = 500$.

(b1), (c1) and (d1), $\beta = 0.5$; in the cases (a2), (b2), (c2) and (d2), $\beta = 0.99$. In these tests, the kinematic viscosity ratios are kept at unity but the two fluids have different densities. The numerical and analytical solutions are shown in Fig. 4. Table 3 also shows whether the source term [i.e. Eq. (19)] is added into LBE in the simulation to cancel the unwanted terms. We can see that neither numerical solutions of $\frac{\rho_1}{\rho_2} = 0.5$ [see Figs. 4(a) and 4(b)] nor those of $\frac{\rho_1}{\rho_2} = 2$ [see Figs. 4(c) and 4(d)] are consistent with the analytical solutions. The incorrect numerical result in Fig. 4(d) is also similar to that obtained in Fig. 9 in Ref. 26. Our simulations further confirm that the simulation in Ref. 26 is correct. In Fig. 4, we can see that the numerical velocities jump near the interface vicinity and they are not continuous as the analytical

Table 3. Parameters for the R−K models simulations of parallel flows with different densities ($A = 10^{-4}$, $\tau_1 = \tau_2 = 1$ and $G' = 1.5 \times 10^{-8}$).

Case	α_1	α_2	$\frac{\rho_1}{\rho_2} = \frac{1-\alpha_2}{1-\alpha_1}$	β	G_1	G_2	Eliminate unwanted terms?
(a1)	0.2	0.6	0.5	0.5	0	G'	No
(b1)	0.2	0.6	0.5	0.5	G'	0	No
(c1)	0.6	0.2	2	0.5	0	G'	No
(d1)	0.6	0.2	2	0.5	G'	0	No
(a2)	0.2	0.6	0.5	0.99	0	G'	No
(b2)	0.2	0.6	0.5	0.99	G'	0	No
(c2)	0.6	0.2	2	0.99	0	G'	No
(d2)	0.6	0.2	2	0.99	G'	0	No
(a3)	0.2	0.6	0.5	0.99	0	G'	Yes
(b3)	0.2	0.6	0.5	0.99	G'	0	Yes
(c3)	0.6	0.2	2	0.99	0	G'	Yes
(d3)	0.6	0.2	2	0.99	G'	0	Yes
(e)	0.9	0.2	8	0.2	G'	G'	No
(f)	0.9	0.2	8	0.2	G'	G'	Yes
(g)	0.2	0.9	0.125	0.2	G'	G'	No
(h)	0.2	0.9	0.125	0.2	G'	G'	Yes

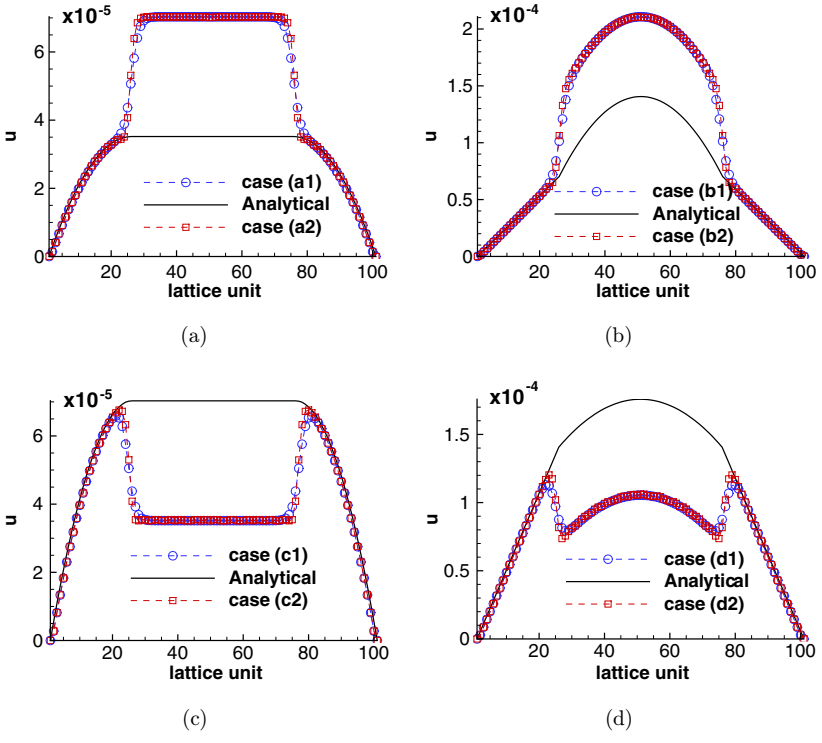

Fig. 4. (Color online) Velocity profiles for cases with $M = 1$, density ratio $\frac{\rho_1}{\rho_2} = 0.5$ [(a) and (b)] and $\frac{\rho_1}{\rho_2} = 2$ [(c) and (d)]. The unit of the velocity is $l.u./t.s$.

solutions are. This is easy to understand because as mentioned above, the undesired term $u_x\partial_y(\rho_1)$ is not negligible. It plays an important role in the significant velocity jump near the interface in the simulations and is not physical.

In Fig. 4(a), we can see that there are very minor discrepancies between the results obtained from cases (a1) and (a2), which have different β. The discrepancies are only limited in the interface vicinity. For case (a1) and (a2), the interface thickness are approximately 6 $l.u.$ and 4 $l.u.$, respectively. In Figs. 4(b)−4(d), we also see that the parameter β only affects the interfacial thickness. Here, different parameter β has very minor effect on the whole numerical result. It is noted that for a higher density ratio case, when the interface is too thin, the numerical instability may appear.

In the above, we mentioned that using the source term, i.e. Eq. (19), the unwanted terms in Eq. (17) may be eliminated and the correct N−S equations for each component are recovered. To demonstrate our argument on the extra terms more clearly, we would like to assess whether the numerical result is correct if the unwanted terms in Eq. (17) can be eliminated. In the cases (a3) to (d3), which are listed in Table. 3, the source terms are added into the LBE. The results of (a3), (b3), (c3) and (d3) are shown in Fig. 5. We can see that now the results agree well with the analytical solutions except very small-velocity jumps in the interfacial region.

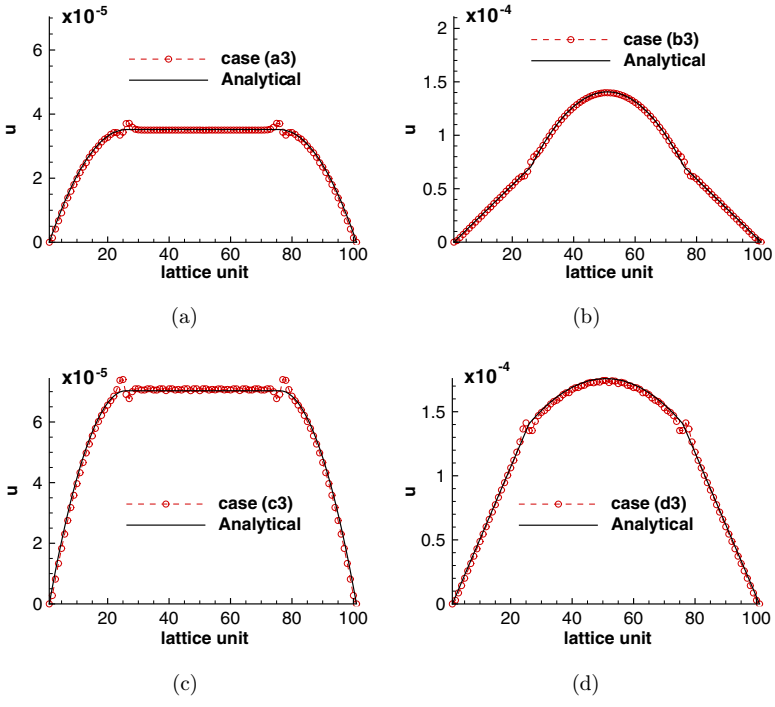

Fig. 5. (Color online) Comparison of the velocity profiles obtained from cases (a3), (b3), (c3), (d3) and the corresponding analytical solutions. Density ratio $\frac{\rho_1}{\rho_2} = 0.5$ [(a) and (b)] and $\frac{\rho_1}{\rho_2} = 2$ [(c) and (d)]. In this simulations, $\tau_1 = \tau_2 = 1$ and the unwanted terms are eliminated. The unit of the velocity is $l.u./t.s$.

The errors between the LBM result and the analytical one are 1.74%, 1.20%, 1.93% and 1.89% for cases (a3), (b3), (c3) and (d3), respectively. For the velocity profiles of case (c3) and (d3), we notice that there are small-amplitude oscillations in the center region (fluid 1 region). Using a smaller β, which allows thicker interface would eliminate the oscillation.

To illustrate the difference between the simulations with and without the source term, here a residual is defined. As we know, in the final steady state, the following equation for this parallel two-phase flow is expected to be satisfied on each lattice node,

$$\rho_k \nu_k \partial_y^2 u_x + G = 0. \tag{23}$$

However, usually there is a residual in numerical simulations, which means the right hand side of the above equation may not be zero. Here the residual is defined as $\theta = \rho_k \nu_k \partial_y^2 u_x + G$. Numerically, the residual at a lattice node (i, j) can be evaluated through $\theta^k_{(i,j)} = \rho_k \nu_k \frac{1}{\delta y^2} [(u_x)_{(i,j+1)} + (u_x)_{(i,j-1)} - 2(u_x)_{(i,j)}] + G_{(i,j)}$ after the numerical results are converged. It is noted that θ has identical unit as G.

The residual of the two simulations for fluid 1 are shown in Fig. 6(a). The original simulation denotes case (b1) and the revised one denotes the simulation with identical parameters as case (b1) but the source term [see Eq. (19)] is added. To illustrate

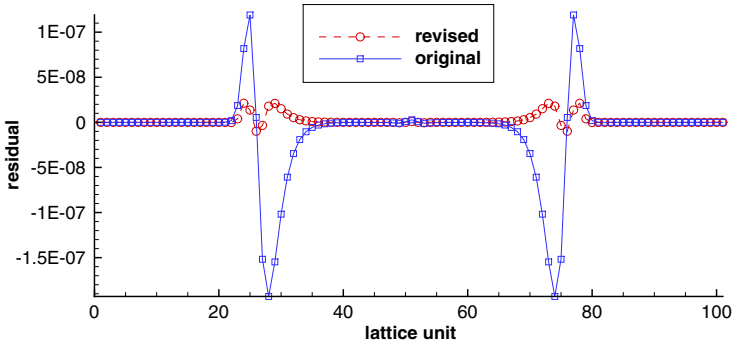

(a)

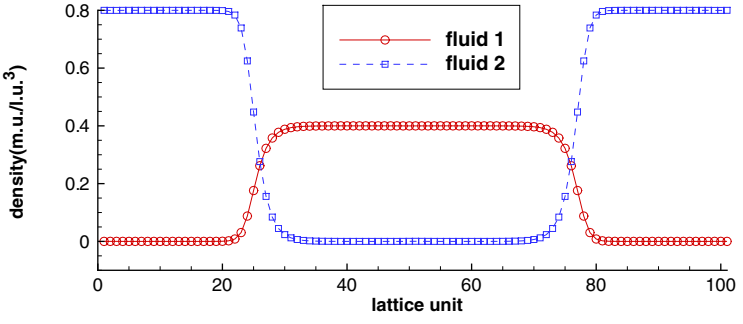

(b)

Fig. 6. (Color online) (a) Residual of fluid 1 for the original simulation (case (b1)), and the revised simulation (case (b1) with the unwanted terms eliminated). (b) density profiles for case (b1).

the interface vicinity clearly, the density profiles for the fluids 1 and 2 are shown in Fig. 6(b). In the figure, we can see that the residual of the original simulation in the interfacial region is much larger than that of the revised one. On the other hand, from Eq. (21), we know that due to the unwanted terms

$$U_x^k = (\tau_k - 0.5)\left[\frac{c^2}{3} - (c_s^k)^2\right]\partial_y(u_x\partial_y\rho_k), \tag{24}$$

is involved in the original simulation, the residual of the original one is expected to be larger than the revised one. Hence, Fig. 6(a) confirmed our analysis.

In the meantime, it is also noticed that for the revised simulation, in the interface vicinity, the residual are still not exactly to be zero. This is attributed to the error introduced by the finite difference scheme.

We further simulated cases with higher density contrast (i.e. cases (e) to (h)). The parameters of cases (e) to (h) are listed in Table 3. It is noted that in the simulations of case (f) and (h), the unwanted terms are eliminated. Here $\beta = 0.2$ is used because a larger β (e.g. $\beta = 0.3$) would lead to numerical instability. Comparisons between the cases with and without the added source term are shown in Fig. 7. Results of cases (f)

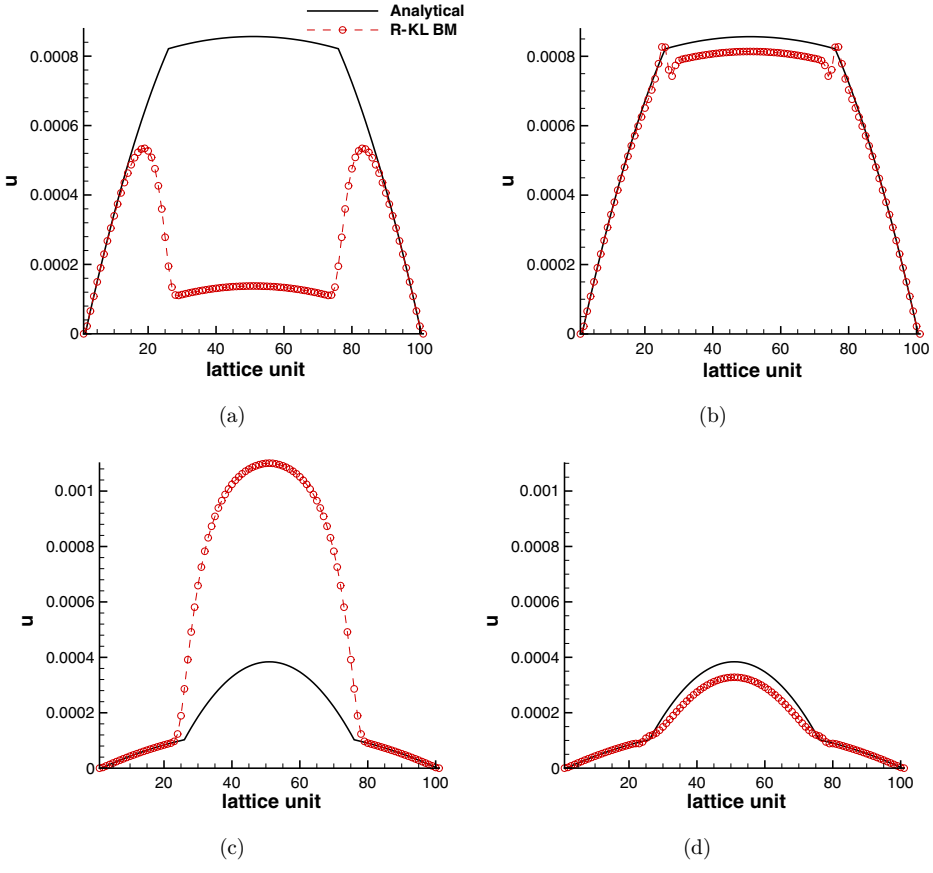

Fig. 7. (Color online) Velocity profiles for cases with different densities and $G = 1.5 \times 10^{-8}$. (a) $\alpha_1 = 0.9, \alpha_2 = 0.2, \frac{\rho_1}{\rho_2} = \frac{0.8}{0.1}$; (b) the source term [see Eq. (19)] is added in the simulation and parameters are identical as those in (a); (c) $\alpha_1 = 0.2, \alpha_2 = 0.9, \frac{\rho_1}{\rho_2} = \frac{0.1}{0.8}$; (d) the source term [see Eq. (19)] is added in the simulation and parameters are identical as those in (c).

and (h) are more consistent with the analytical solutions. They are much better than results of corresponding cases (e) and (g), which are simulated without adding the source term. The errors [see Eq. (22)] in cases (f) and (h) are 4.09% and 14.05%, respectively. Hence, if the unwanted terms can be canceled, the R−K model is able to simulate the cases with density difference significantly better.

In Fig. 8, the total residuals $\theta_{(i,j)} = \sum_k \theta^k_{(i,j)}$ for the simulations of case (g) and (h) are shown. In the simulation of case (h), the source term is added. We can see that again, the residual of the original simulation (case (g)) is much larger than that of the revised one (case (h)) in the interface vicinity. Hence, the effect of our source term is significant.

It is also noted that error in cases of higher density contrast [e.g. 14.05% in cases (h)] is larger than those of lower density ratio cases (refer to Fig. 5). Using a larger computational domain is helpful to decrease the numerical error. For the case (h),

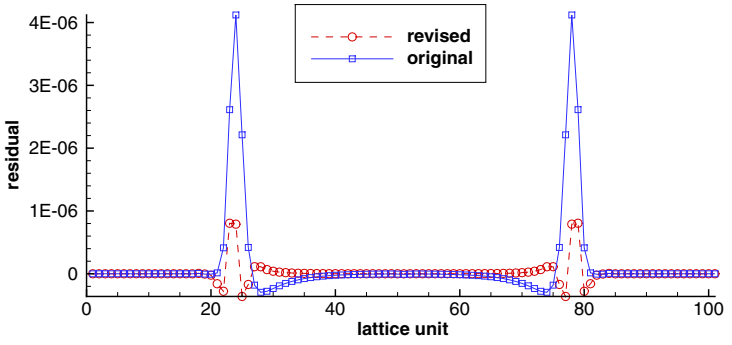

(a)

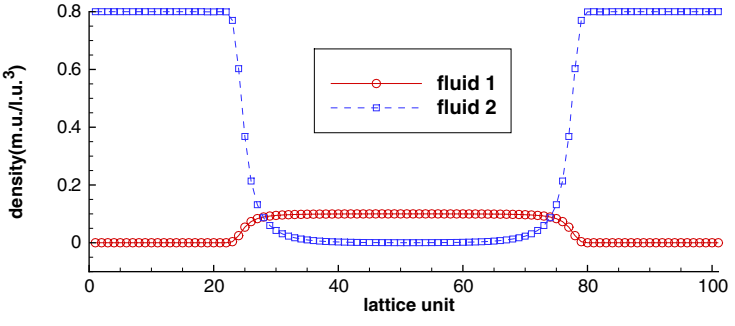

(b)

Fig. 8. (Color online) (a) Total residuals for fluid 1 and 2 in the original simulation (case (g)) and the revised simulation (case (h)), (b) density profiles for case (g).

when the width of the channel is represented by $200\,l.u.$, $300\,l.u.$ and $400\,l.u.$, the numerical errors are 9.14%, 7.03% and 5.88%, respectively. Hence, the error decreases with the grid refinement.

Theoretically, the source term should correct the error completely. For the lower density contrast, from results of cases (a3)−(d3), we conclude that the source term almost corrects the error completely because the numerical results are very accurate. However, when the density contrast is high, the numerical error becomes larger. This results from the finite difference scheme we used. As we know, when the density contrast increases, if the interface thickness is limited, the density gradient would increase. Under the circumstances, when the gradient is evaluated, larger numerical error seems unable to avoid.

To demonstrate the above opinion, simulations of cases with lower and higher density contrast were performed and the results are listed in Table 4. Density ratio in cases (i1), (i2) and (i3) are $\kappa = 0.5$. Density ratio in cases (i4), (i5) and (i6) are higher ($\kappa = 0.125$). When $\beta = 0.3$ (case (i6)), numerical instability appears and the result is not evaluated. From the table, we can see that when β increases, the interface becomes thinner and the magnitudes of unwanted terms and the residual also

Table 4. Results for the R−K models simulations of parallel flows with different densities (In all cases, the computational domain is 10×100 and the source term is added into LBE. $A = 10^{-4}$, $\tau_1 = \tau_2 = 1$, $G = 1.5 \times 10^{-8}$, η is interface thickness, U_x^k denotes unwanted terms for component k).

Case	α_1	α_2	$\frac{\rho_1}{\rho_2} = \frac{1-\alpha_2}{1-\alpha_1}$	β	η (l.u.)	Error E	$\lvert U_x^1\rvert_{\max}$	$\lvert U_x^2\rvert_{\max}$	$\lvert\theta_{i,j}^1\rvert_{\max}$	$\lvert\theta_{i,j}^2\rvert_{\max}$
(i1)	0.04	0.52	$\frac{0.48}{0.96} = 0.5$	0.2	≈ 25	1.41%	$5.0e{-8}$	$2.1e{-8}$	$0.15e{-8}$	$2.1e{-8}$
(i2)	0.04	0.52	0.5	0.5	≈ 11	0.69%	$2.5e{-7}$	$1.0e{-7}$	$0.3e{-7}$	$1.2e{-7}$
(i3)	0.04	0.52	0.5	0.9	≈ 6	0.63%	$6.0e{-7}$	$2.1e{-7}$	$1.3e{-7}$	$5.4e{-7}$
(i4)	0.04	0.88	$\frac{0.12}{0.96} = 0.125$	0.05	≈ 30	26.7%	$1.1e{-8}$	$9.1e{-8}$	$1.5e{-8}$	$3.7e{-8}$
(i5)	0.04	0.88	0.125	0.2	≈ 12	15.3%	$1.08e{-7}$	$9.3e{-7}$	$0.5e{-7}$	$6.7e{-7}$
(i6)	0.04	0.88	0.125	0.3	—	—	—	—	—	—

increase. However, for cases with different β, smaller residual does not necessary mean smaller numerical error E. Here we can see that error E decreases with β in both the cases of $\kappa = 0.5$ and $\kappa = 0.125$. Hence, to get a more accurate result with smaller E, for a specific case, a larger β is preferred if the numerical instability does not appear.

Smaller β, which means thicker interface, may improve the accuracy of evaluation on the source term when the finite difference scheme is used. However, the numerical error E does not decrease when the interface becomes thicker. A possible reason is that physically, a thicker interface means diffusion between the two components becomes more serious. In the R−K model, which is applied to simulate immiscible two-phase flows, serious diffusion would induce a large numerical error.

The distribution of the unwanted terms and residuals in cases (i2) and (i5) are shown in Fig. 9. In cases (i2) and (i5), the interface thicknesses are almost identical in the two cases. From Fig. 9 and Table 4, we can see that in the case with high-density contrast [case (i5)], the maximum magnitudes of the unwanted terms and residual for fluid 2 are much larger than those in the case of low density contrast. In a whole, the case with high-density contrast shows a larger numerical error.

We conclude that, to get accurate results, a thinner interface is preferred. For a thin interface, the numerical evaluation of the source term (including density

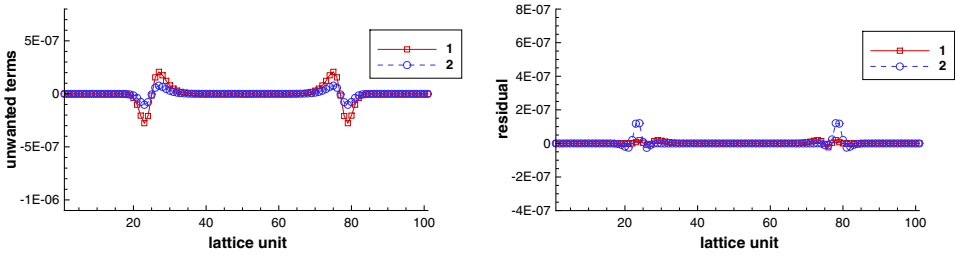

(a) (b)

Fig. 9. (Color online) (a) Unwanted terms U_x^k and (b) residual $\theta_{i,j}^k$ for each component (fluid 1: $k = 1$, fluid 2: $k = 2$) in the simulation of case (i2); (c) unwanted terms U_x^k and (d) residual $\theta_{i,j}^k$ for each component (fluid 1: $k = 1$, fluid 2: $k = 2$) in the simulation of case (i5).

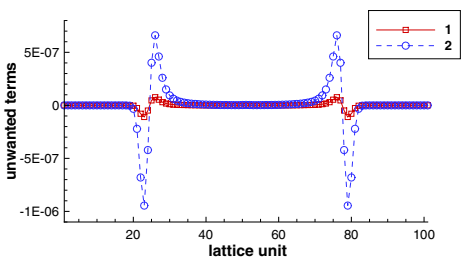

(c)

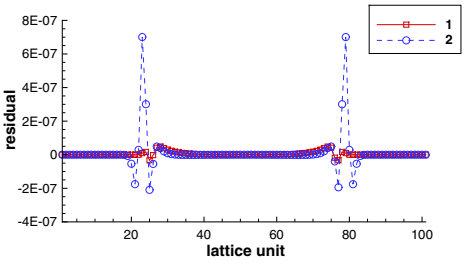

(d)

Fig. 9. (*Continued*)

gradient) for a case with higher density contrast is not as accurate as that in a case with lower density contrast. Hence, for a case with higher density contrast, the numerical error is larger than that in the case with lower density contrast.

4. Conclusion

In this paper, we clarify confusion in the LBM community about using the R−K model for high-density-ratios. The analysis shows that the color-gradient model[16,20,23,25] introduces extra undesired terms into the recovered N−S equations. Because the unwanted terms can be dropped for two components with identical densities, the R−K model is accurate under those circumstances.

In the simulations of spherical bubbles and droplets, the unwanted terms seem not important and the results are not affected much. However, in the simulations of parallel two fluid flows in a channel, the undesired terms in Eq. (16) affect the numerical result significantly. If the unwanted terms in the recovered momentum equation cannot be eliminated, the R−K model only gives poor numerical solution for two-phase flows with different densities.

To eliminate the unwanted terms, the source terms including derivatives have to be evaluated using finite difference scheme. In the R−K model, to get more accurate results, thinner interfaces are preferred. In the cases of lower density contrast, the source term can be evaluated more accurately than cases with higher density contrast and hence the results would be better. Under the circumstance of high-density contrast, if the interface is very thin (β is closer to unity), numerical instability may appear. Our test shows that the scheme we proposed only works well for cases of low density contrast.

Acknowledgments

This work was supported by the National Science Foundation of China (NSFC, Grant No. 10802085).

References

1. R. Scardovelli and S. Zaleski, *Annu. Rev. Fluid Mech.* **31**, 567-603 (1999).
2. H. H. Liu, A. Valocchi and Q. J. Kang, *Phys. Rev. E*, **85**, 046309 (2012).
3. M. C. Sukop and D. T. Thorne, *Lattice Boltzmann Modeling: An Introduction for Geoscientists and Engineers*, 1st edn. (Springer, Heidelberg, Berlin, New York, 2006).
4. K. Langaas and P. Papatzacos, *Trans. Porous Media* **45**, 241 (2001).
5. C. Pan, M. Hilpert and C. T. Miller, *Wat. Resour. Res.* **40**, W01501 (2004).
6. H. Huang and X.-Y. Lu, *Phys. Fluids* **21**, 092104 (2009).
7. J. J. Huang, C. Shu, Y. T. Chew and H. W. Zheng, *Int. J. Mod. Phys. C* **18**, 492 (2007).
8. Z.-T. Li, G.-J. Li, H.-B. Huang and X.-Y. Lu, *Int. J. Mod. Phys. C* **22**, 729 (2011).
9. D. Chiappini, G. Bella, S. Succi and S. Ubertini, *Int. J. Mod. Phys. C* **20**, 1803 (2009).
10. X. Shan and H. Chen, *Phys. Rev. E* **47**, 1815 (1993).
11. M. R. Swift, E. Orlandini, W. R. Osborn and J. M. Yeomans, *Phys. Rev. E* **54**, 5041 (1996).
12. D. H. Rothman and J. M. Keller, *J. Stat. Phys.* **52**, 1119 (1988).
13. H. Huang, L. Wang and X.-Y. Lu, *Comput. Math. Appl.* **61**, 3606 (2011).
14. H. Huang, M. Krafczyk and X.-Y. Lu, *Phys. Rev. E* **84**, 046710 (2011).
15. A. K.Gunstensen, D. H. Rothman, S. Zaleski and G. Zanetti, *Phys. Rev. A* **43**, 4320 (1991).
16. D. Grunau, S. Chen and K. Eggert, *Phys Fluids A: Fluid Dynam* **5**, 2557 (1993).
17. M. Latva-Kokko and D. H. Rothman, *Phys. Rev. E* **72**, 046701 (2005).
18. S. Leclaire, M. Reggio and J.-Y. Trépanier, *Appl. Math. Model.* **36**, 2237 (2012).
19. M. Latva-Kokko and D. Rothman, *Phys. Rev. Lett.* **98**, 254503 (2007).
20. T. Reis and T. N. Phillips, *J. Phys. A: Math. Theor.* **40**, 4033 (2007).
21. S. V. Lishchuk, C. M. Care and I. Halliday, *Phys. Rev. E* **67**, 036701 (2003).
22. H. Liu and Y. Zhang, *Phys. Fluids* **23**, 082101 (2011).
23. J. Tölke, M. Krafczyk, M. Schulz and E. Rank, *Philos. Trans. A: Math. Phys. Engrg. Sci.* **360**, 535 (2002).
24. S. Leclaire, M. Reggio and J.-Y. Trépanier, *Comput. Fluids* **48**, 98 (2011).
25. J. Tölke, Gitter-Boltzmann-Verfahren zur Simulation von Zweiphasenströmungen. Ph.D. Thesis, Lehrstuhl Bauinformatik, TU M̈unchen, M̈unchen (2001).
26. G. Rannou, Lattice-Boltzmann Method and Immiscible Two-phase Flow, Master's Thesis, Georgia Institute of Technology (2008).
27. X. Y. He, Q. S. Zou, L. S. Luo and M. Dembo, *J. Stat. Phys.* **87**, 115 (1997).